

Electronic Supplementary Information for

**Flow-induced structure and properties of multiwall carbon
nanotube/polydimethylsiloxane composites**

Ran Niu,^{a,b} Jiang Gong,^{a,b} Donghua Xu,^{a,*} Tao Tang^a and Zhao-Yan Sun^{a,*}

^a State Key Laboratory of Polymer Physics and Chemistry, Changchun Institute of Applied Chemistry, Chinese Academy of Sciences, Changchun 130022, P. R. China

^b University of Chinese Academy of Sciences, Beijing 100039, P. R. China

*To whom correspondence should be addressed.

Tel.: +86 (0) 431 85262896.

Fax: +86 (0) 431 85262969.

E-mail: dhxu@ciac.ac.cn and zysun@ciac.ac.cn

Fig. S1: TEM images and length distributions of MWNTs	3
Figs. S2 and S3: Viscosity and normal stress difference measured by different geometries	3
Figs. S4–S6: Frequency sweep results of MWNT/PDMS composites.....	5
Figs. S7 and S8: Influence of PDMS molecular weight on the rheological properties of MWNT/PDMS composites	8
Fig. S9: Influence of aspect ratio of MWNT on the ΔN of MWNT/PDMS composites	10
Fig. S10: Normal stress differences versus shear rate for 16 wt % MWNT2/P6k measured by different geometries	10
Figs. S11–S14: Influence of MWNT concentration on the viscosity of MWNT/PDMS composites	11
Fig. S15: Viscosity of 0.5 wt % MWNT2/P63k under different heights of gap.....	14
Figs. S16–S18: Influence of MWNT concentration on the ΔN of MWNT/PDMS composites	15
Figs. S19–S23: Structural change under shear of low concentration MWNT/PDMS composites	18
Figs. S24 and S25: Normal stress differences of 1 wt % MWNT0/P28k and 0.5 wt % MWNT0/P63k composites under different heights of gap	19
Fig. S26: Structures of 0.5 wt % MWNT0/P117k under different heights of gap.....	20
Tables S1 and S2 Mean aggregate size of MWNT/PDMS composites under static ...	21
Fig. S27: Steady shear results of pure PDMS.....	22

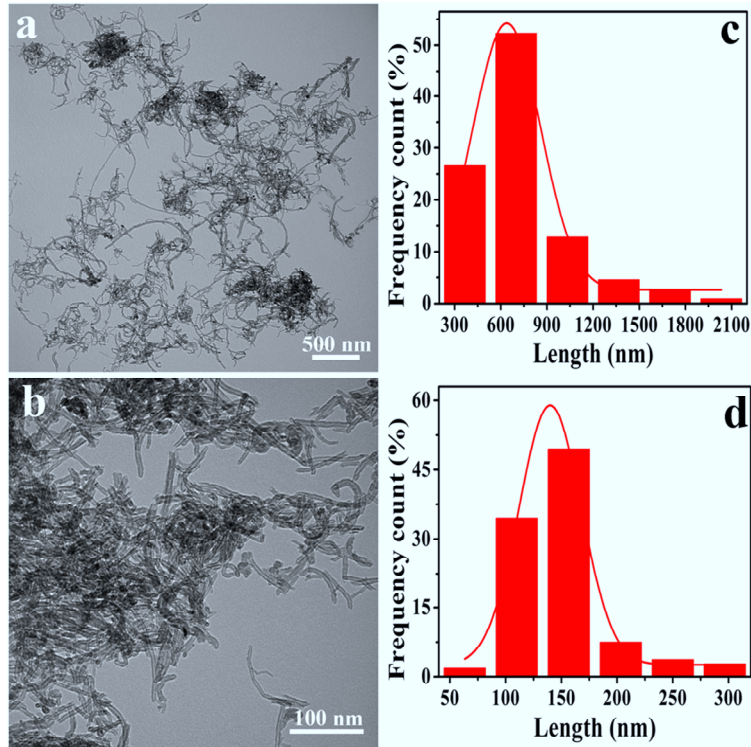


Fig. S1 TEM images and length distributions of MWNT2 (a and c) and MWNT6 (b and d).

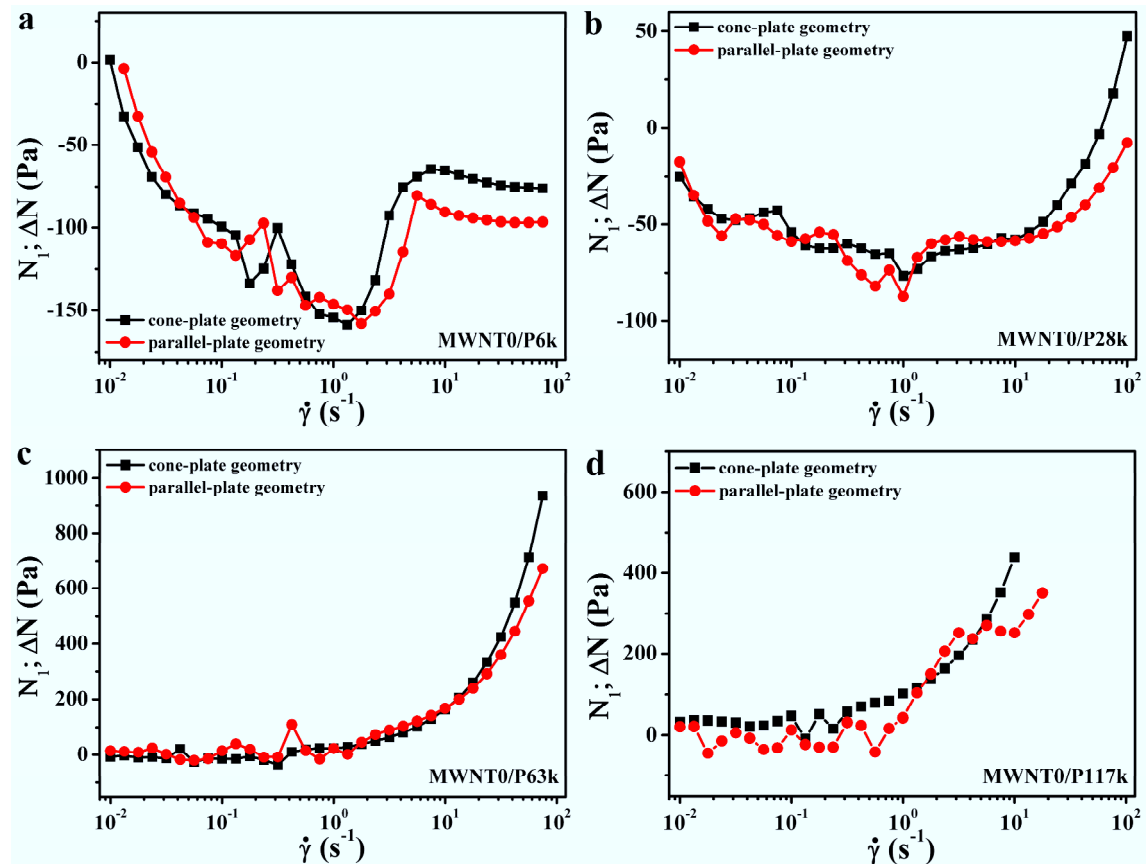


Fig. S2 Normal stress difference (N_1 and ΔN) versus shear rate measured by cone-plate and parallel-plate geometries for 2 wt % MWNT0/PDMS composites.

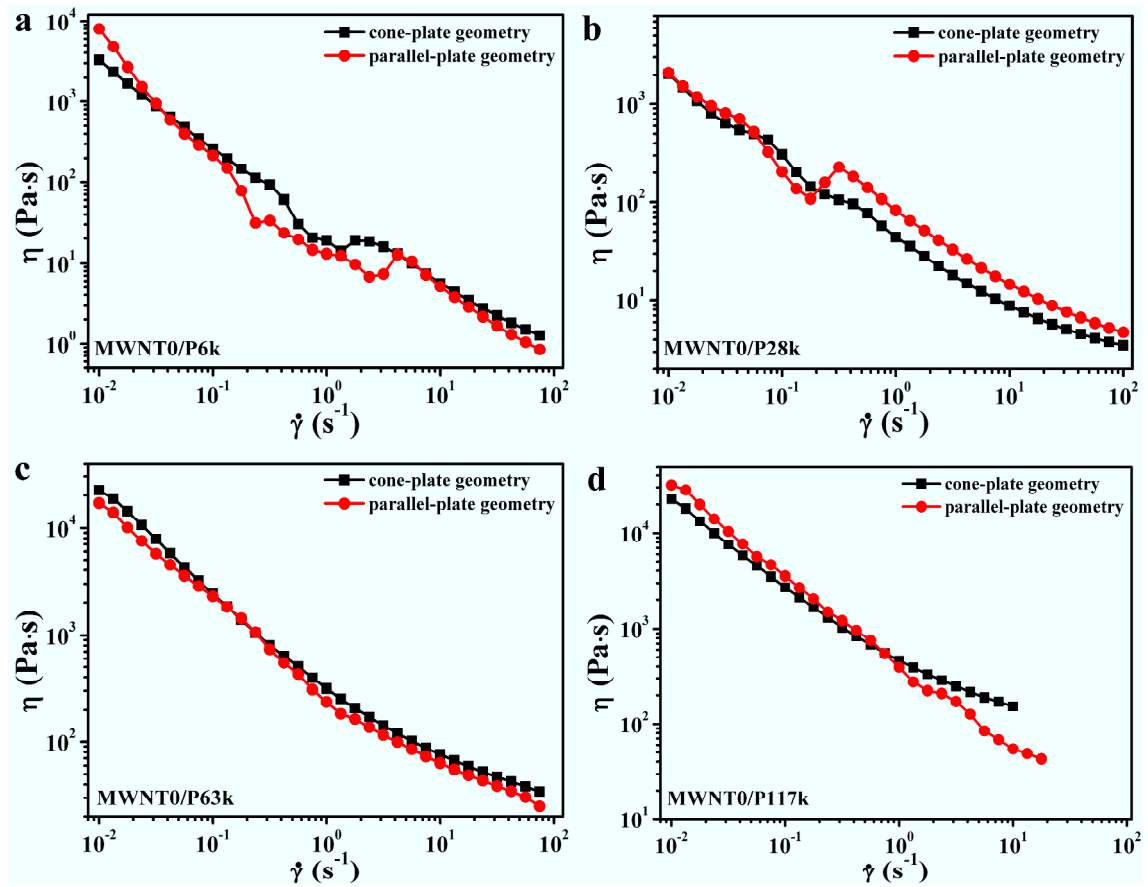


Fig. S3 Viscosity versus shear rate measured by cone-plate and parallel-plate geometries for 2 wt % MWNT0/PDMS composites.

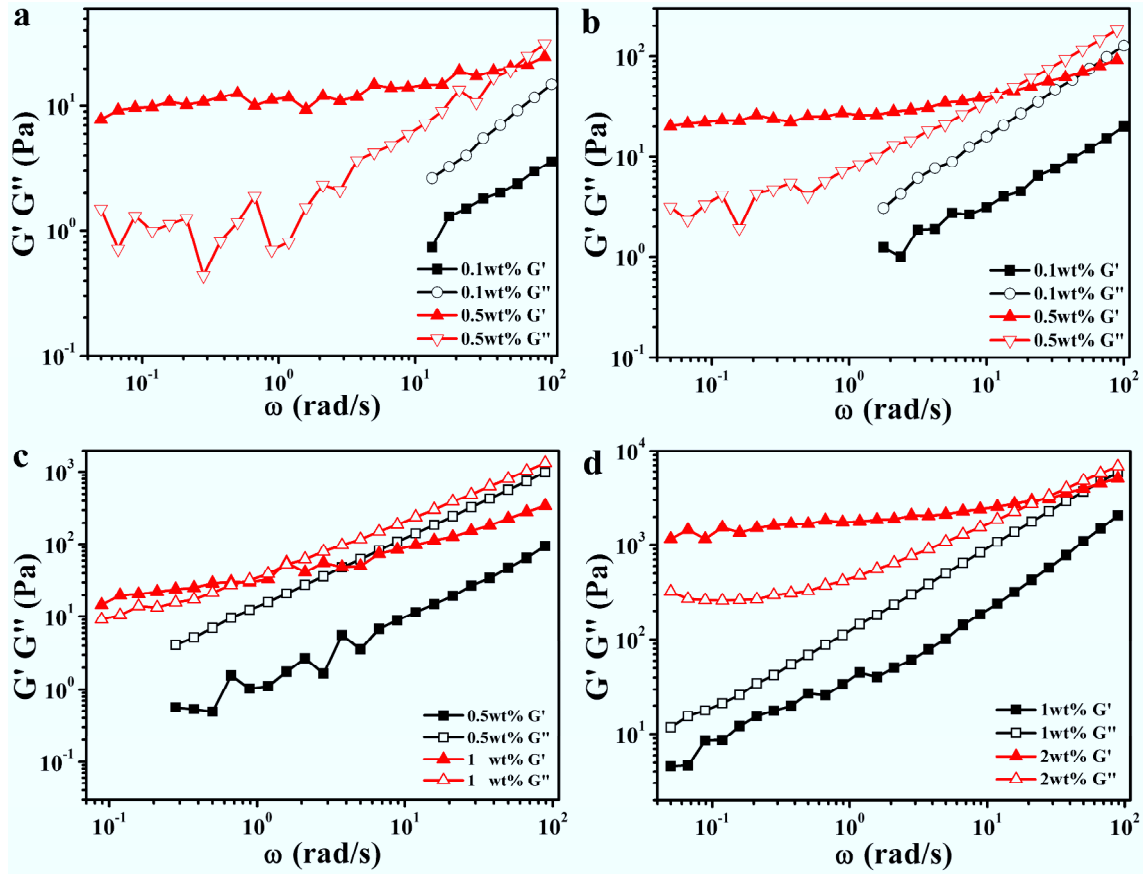


Fig. S4 Frequency sweep results of MWNT0/P6k (a), MWNT0/P28k (b), MWNT0/P63k (c) and MWNT0/P117k composites (d).

For 0.5 wt % MWNT0/P6k and 0.5 wt % MWNT0/P28k, the storage modulus (G') is larger than loss modulus (G''), indicating the formation of network structure.^{S1-S3} However, for 0.1 wt % MWNT0/P6k and 0.1 wt % MWNT0/P28k, the G' and G'' at low frequency cannot be accurately measured as the torque is close to the resolution limit. At high frequency, G'' is larger than G' , suggesting that no network structure forms.^{S1-S3}

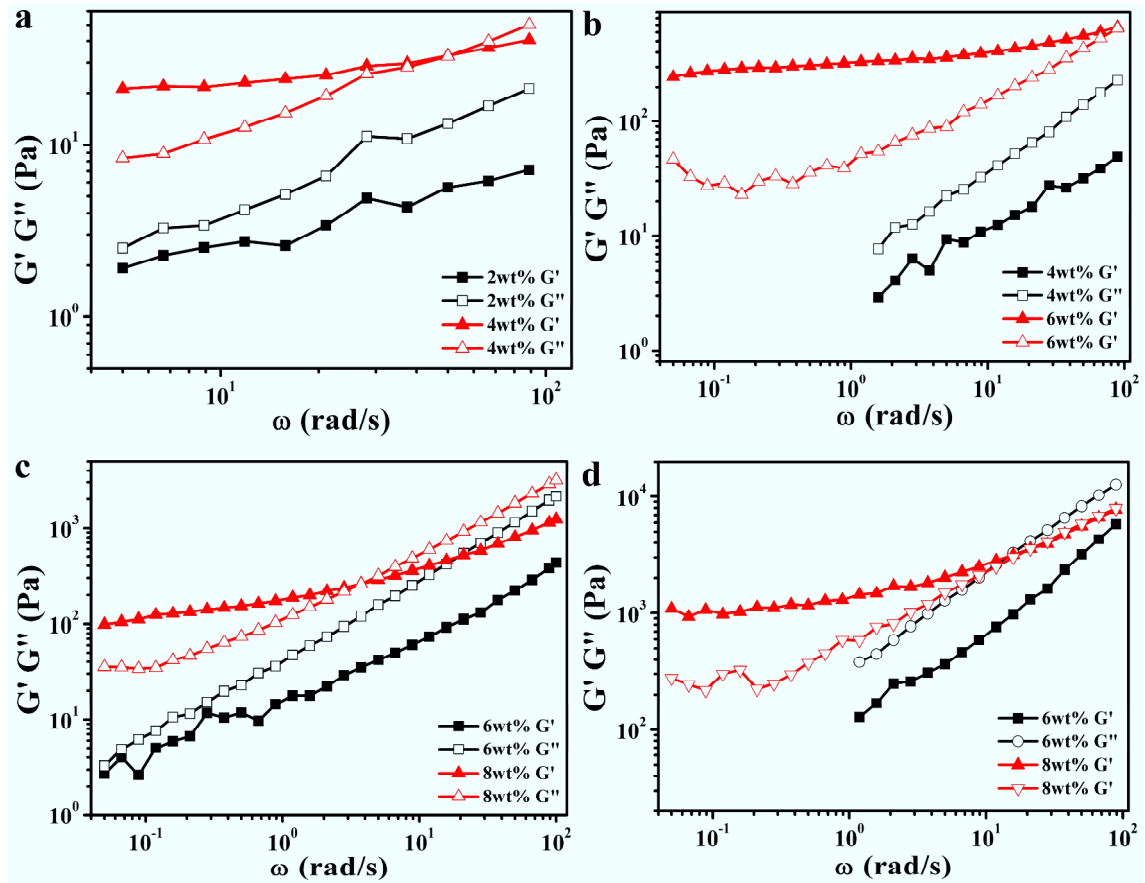


Fig. S5 Frequency sweep results of MWNT2/P6k (a), MWNT2/P28k (b), MWNT2/P63k (c) and MWNT2/P117k composites (d).

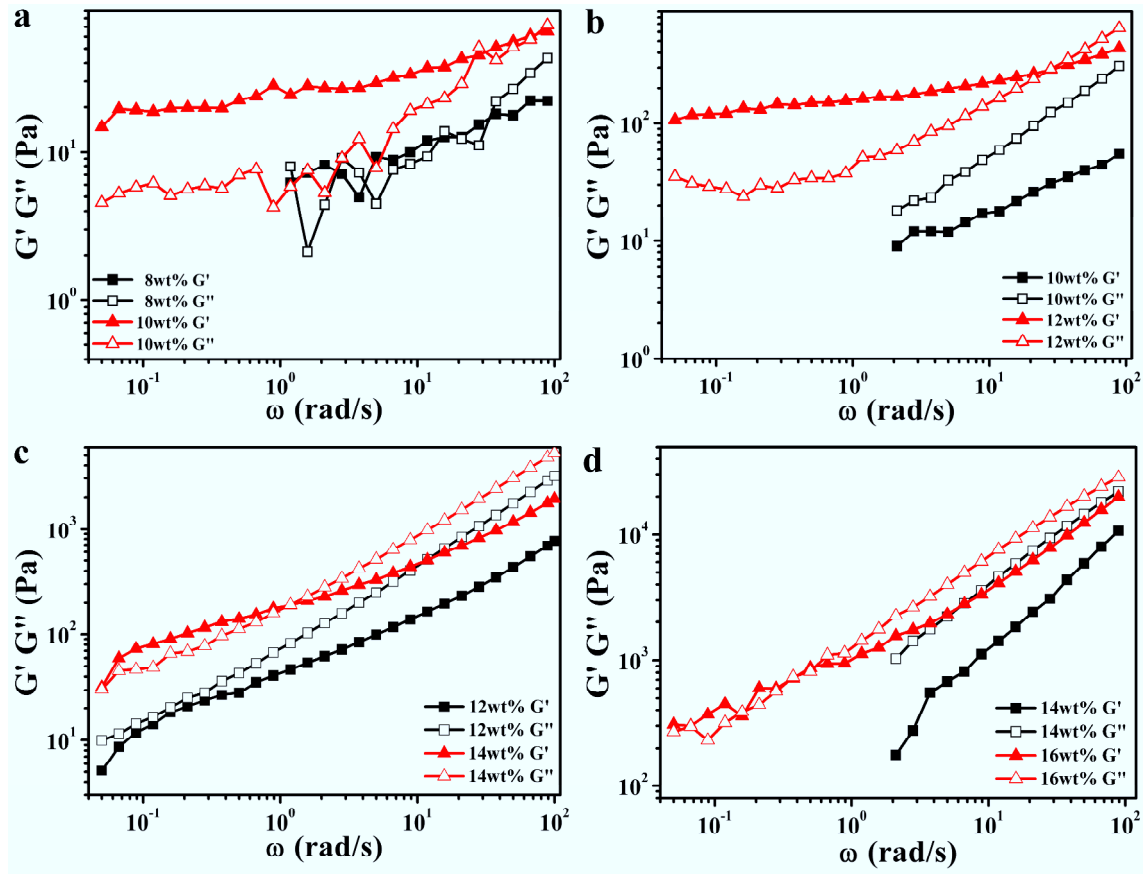


Fig. S6 Frequency sweep results of MWNT6/P6k (a), MWNT6/P28k (b), MWNT6/P63k (c) and MWNT6/P117k composites (d).

Influence of PDMS molecular weight on the rheological properties of MWNT/PDMS composites

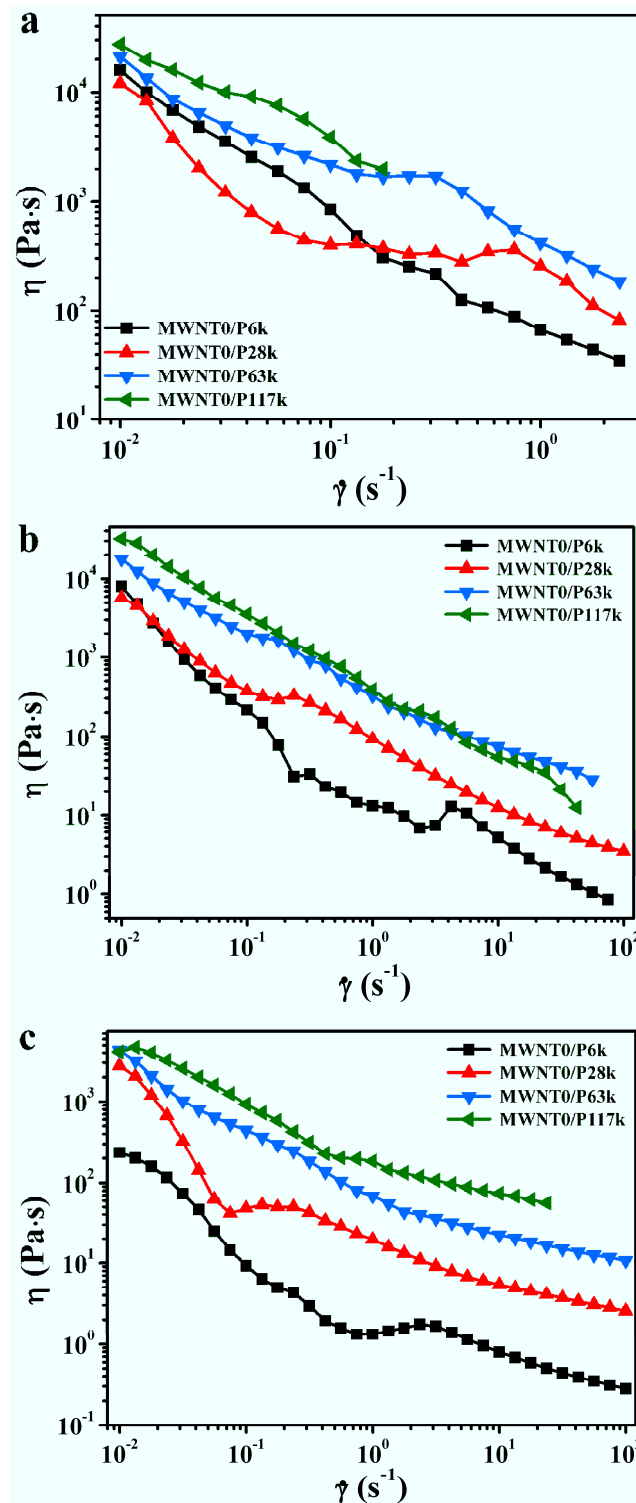


Fig. S7 Viscosity (η) versus shear rate ($\dot{\gamma}$) for MWNT0/PDMS composites with 4 wt % MWNT0 (a), 2 wt % MWNT0 (b) and 1 wt % MWNT0 (c). The gap used in the rheological experiments is about 0.9 mm.

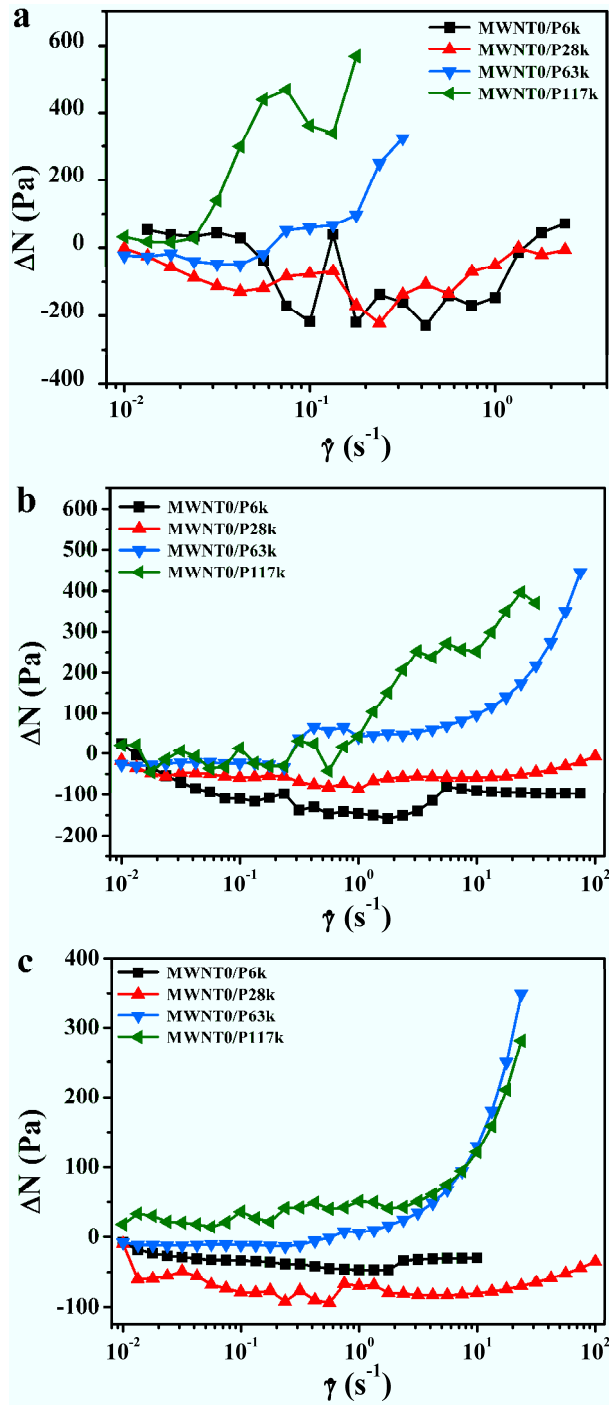


Fig. S8 Normal stress differences (ΔN) versus shear rate ($\dot{\gamma}$) for MWNT0/PDMS composites with 4 wt % MWNT0 (a), 2 wt % MWNT0 (b) and 1 wt % MWNT0 (c). The gap used in the rheological experiments is about 0.9 mm.

Influence of MWNT aspect ratio on the rheological properties of MWNT/PDMS composites

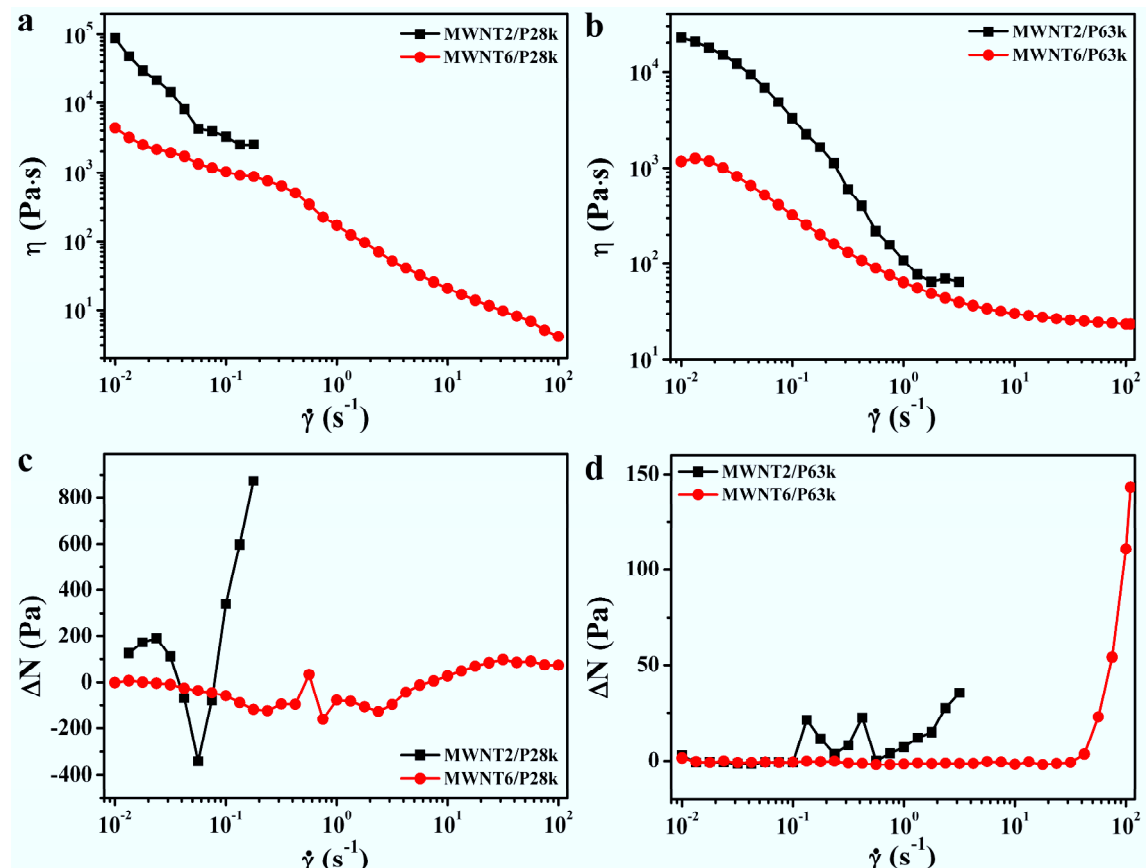


Fig. S9 Viscosity (η) and normal stress differences (ΔN) versus shear rate ($\dot{\gamma}$) for 16 wt % MWNT2/P28k and MWNT6/P28k (a and c); and 16 wt % MWNT2/P63k and MWNT6/P63k composites (b and d). The gap used in the rheological experiments is about 0.9 mm.

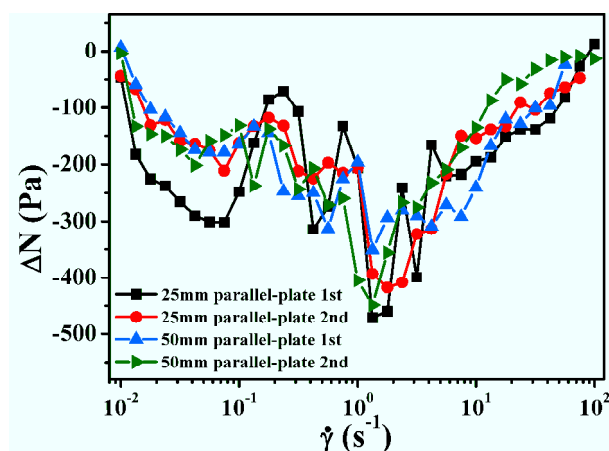


Fig. S10 Normal stress differences (ΔN) versus shear rate for 16 wt % MWNT2/P6k composites measured by different geometries.

Influence of concentration of MWNT on the rheological properties of MWNT/PDMS composites

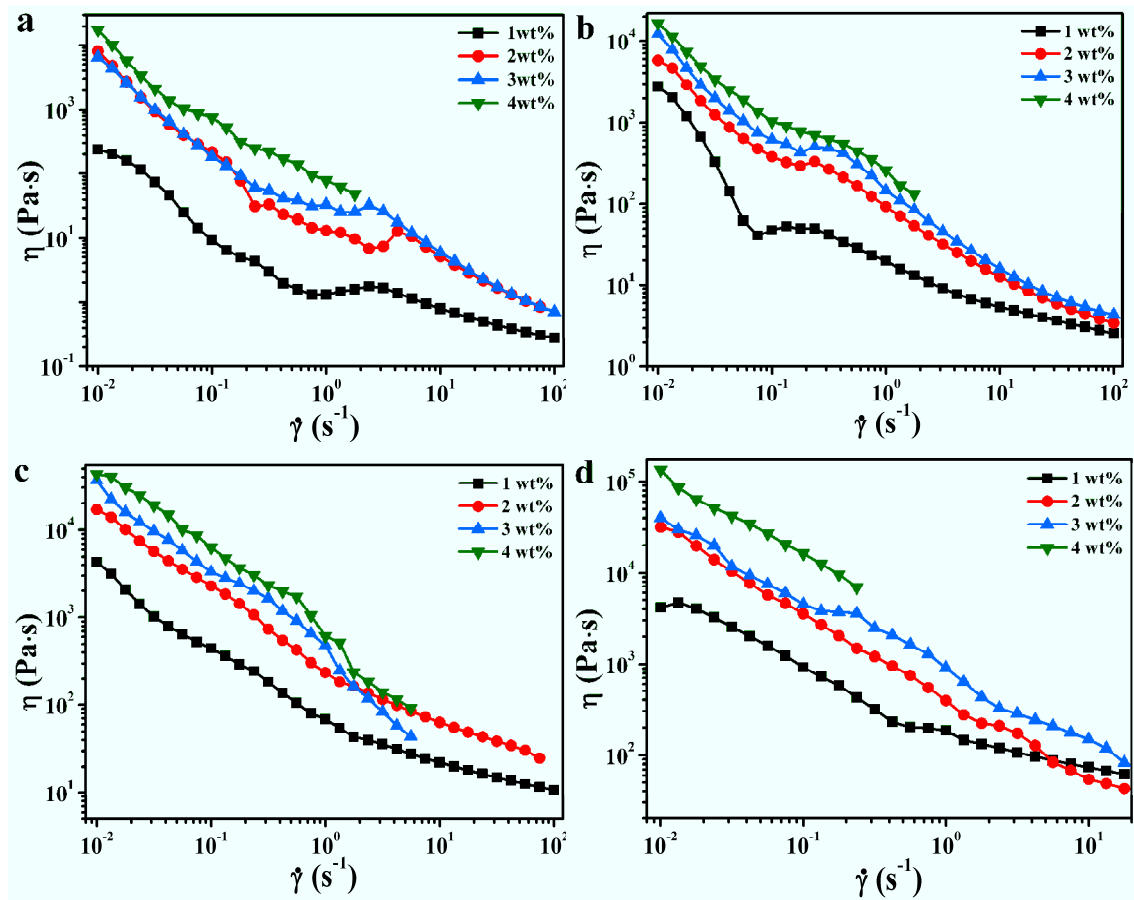


Fig. S11 Viscosity (η) versus shear rate ($\dot{\gamma}$) for MWNT0/P6k (a), MWNT0/P28k (b), MWNT0/P63k (c) and MWNT0/P117k composites (d) with different concentrations of MWNT0. The gap used in the rheological experiments is about 0.9 mm.

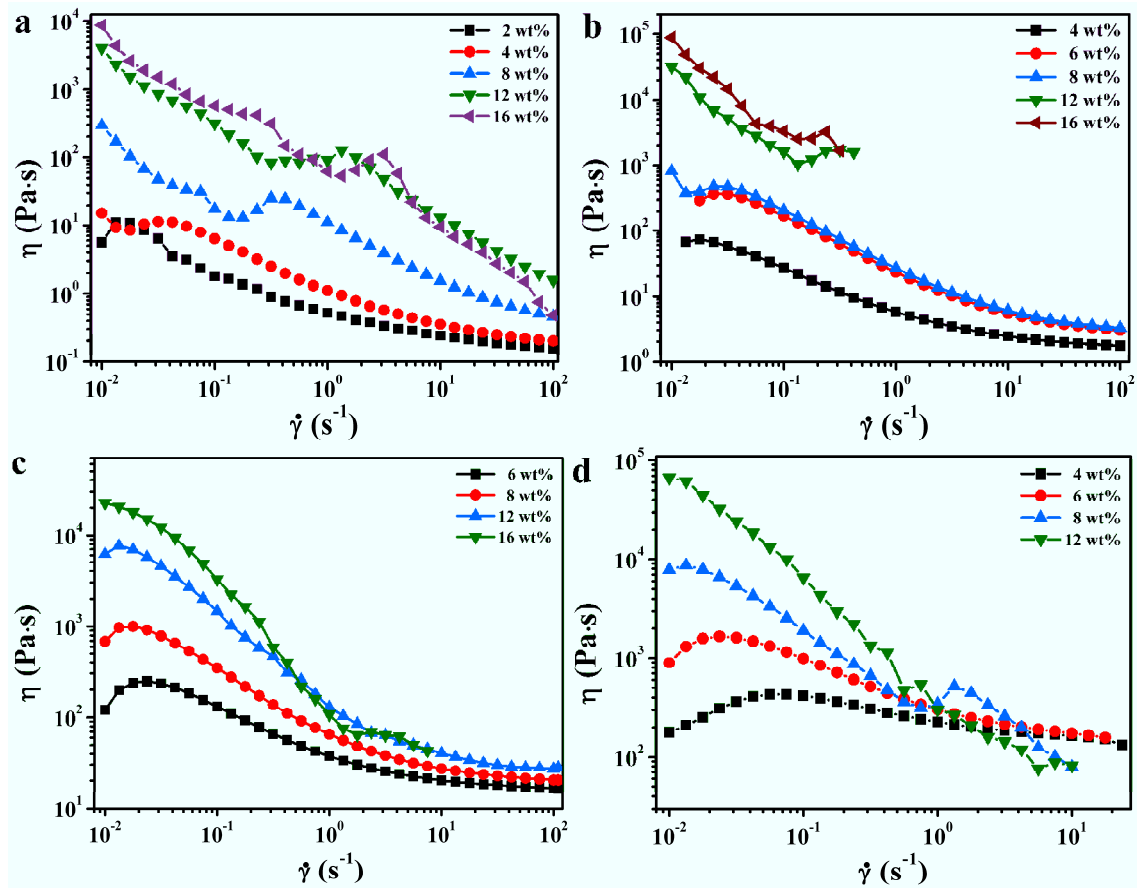


Fig. S12 Viscosity (η) versus shear rate ($\dot{\gamma}$) for MWNT2/P6k (a), MWNT2/P28k (b), MWNT2/P63k (c) and MWNT2/P117k composites (d) with different concentrations of MWNT2. The gap in the rheological experiments is about 0.9 mm.

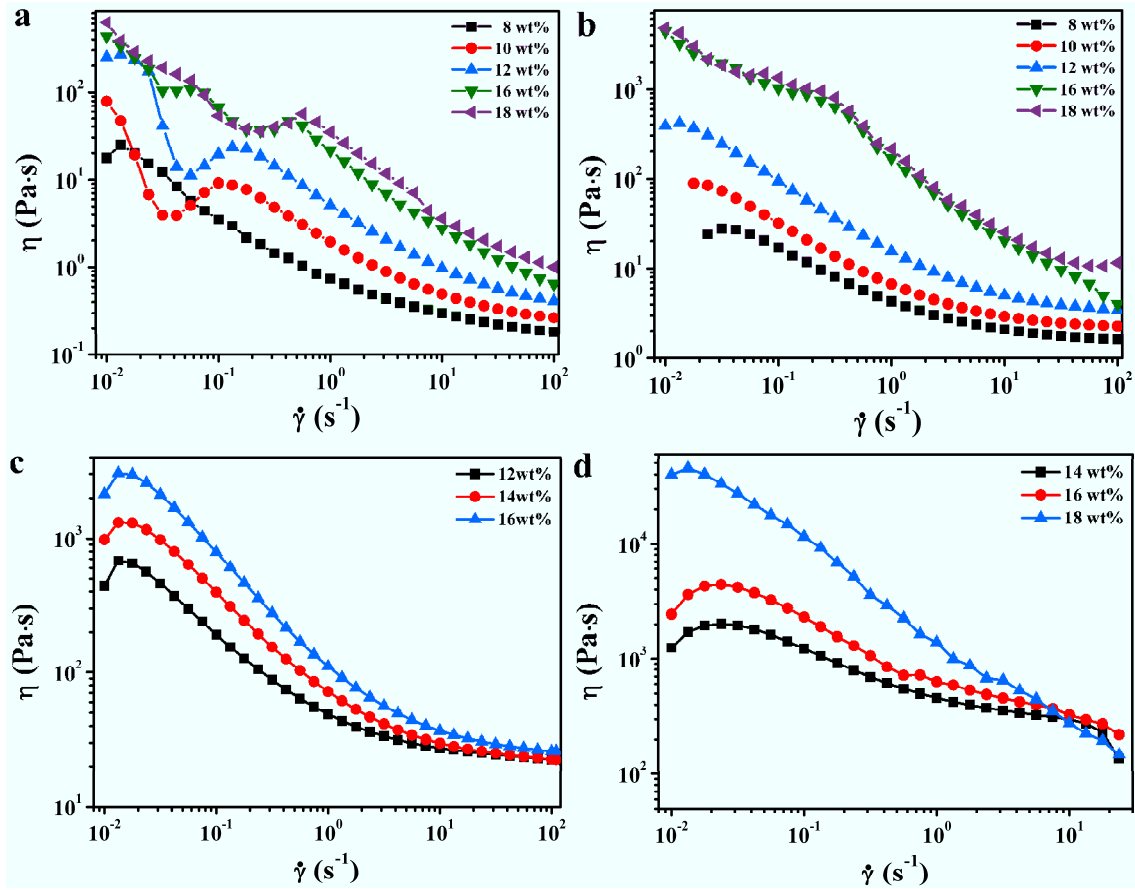


Fig. S13 Viscosity (η) versus shear rate ($\dot{\gamma}$) for MWNT6/P6k (a), MWNT6/P28k (b), MWNT6/P63k (c) and MWNT6/P117k composites (d) with different concentrations of MWNT6. The gap in the rheological experiments is about 0.9 mm.

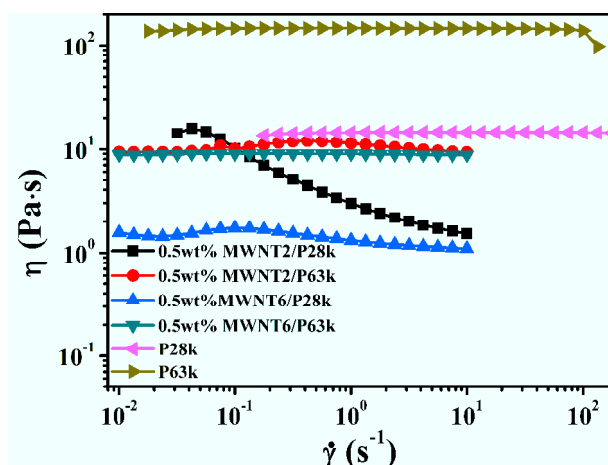


Fig. S14 Viscosity (η) versus shear rate ($\dot{\gamma}$) for MWNT2/P28k, MWNT2/P63k, MWNT6/P28k and MWNT6/P63k composites with 0.5 wt % MWNTs. The gap in the rheological experiments is about 150 μm .

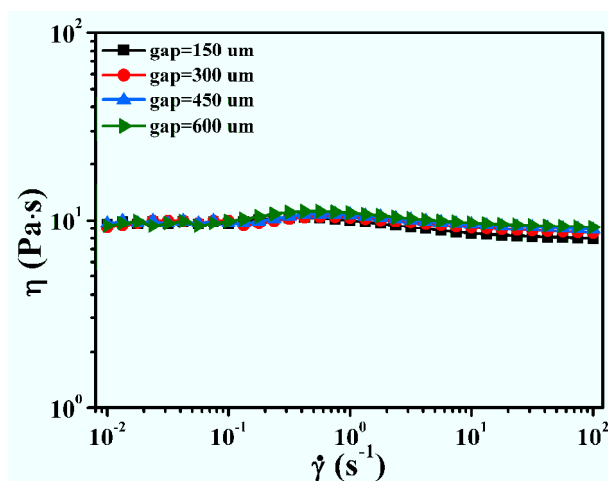


Fig. S15 Viscosity (η) versus shear rate ($\dot{\gamma}$) for 0.5 wt % MWNT2/P63k composites measured at different heights of gap.

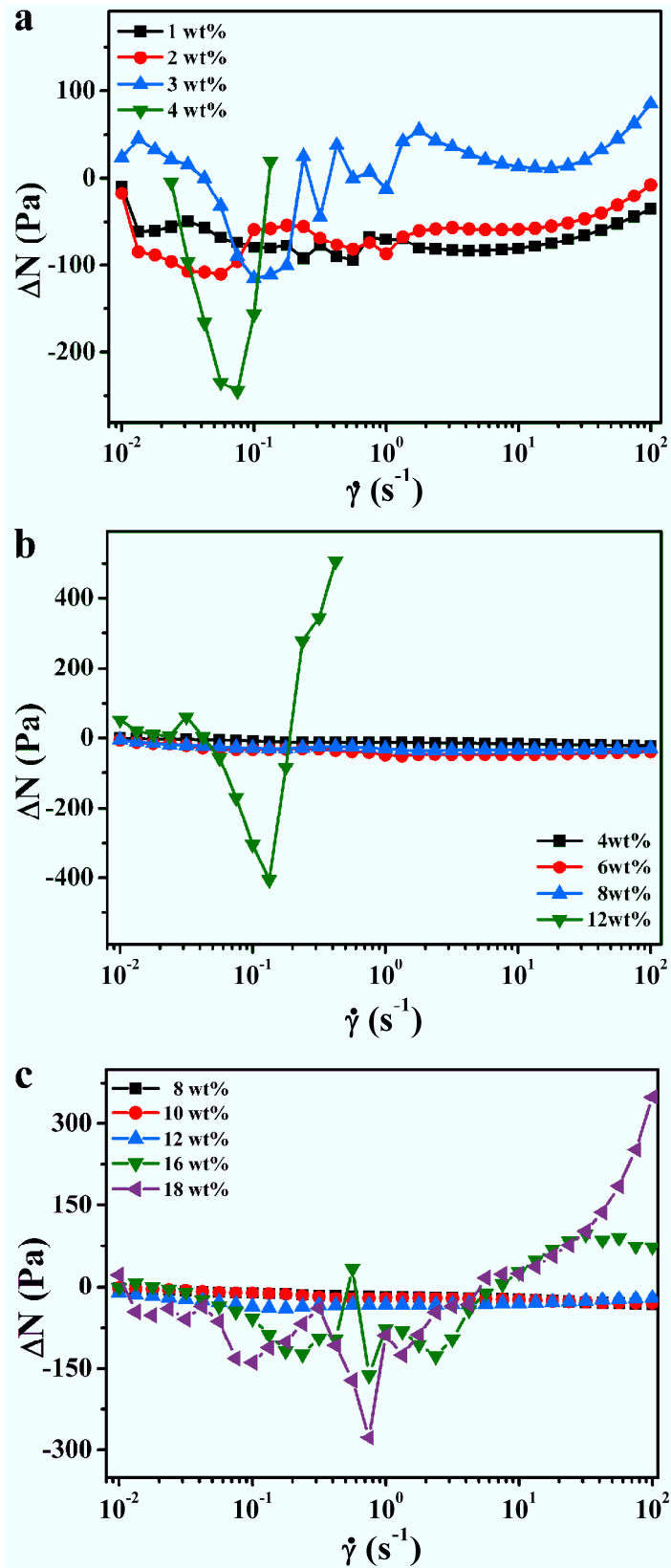


Fig. S16 Normal stress differences (ΔN) versus shear rate ($\dot{\gamma}$) for MWNT0/P28k (a), MWNT2/P28k (b) and MWNT6/P28k composites (c) with different concentrations of MWNT. The gap in the rheological experiments is about 0.9 mm.

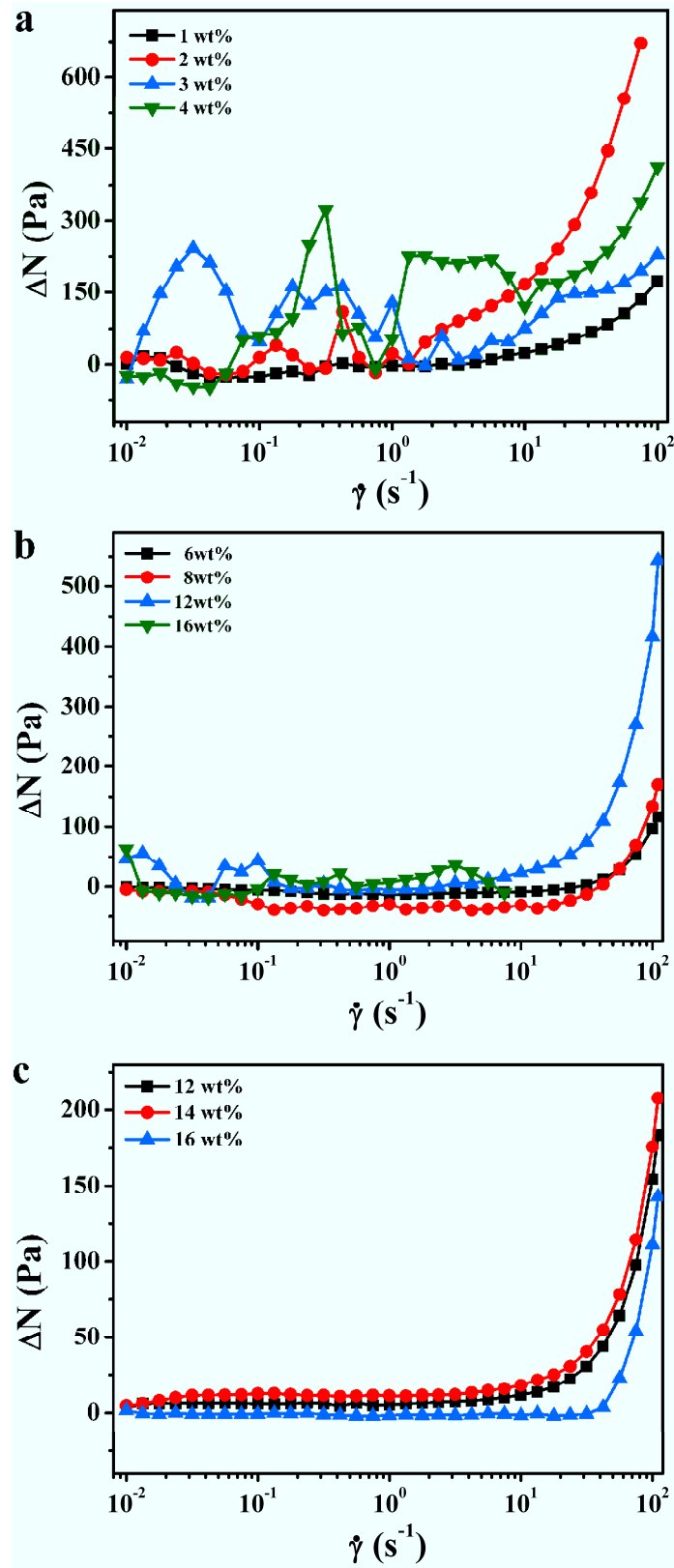


Fig. S17 Normal stress differences (ΔN) versus shear rate ($\dot{\gamma}$) for MWNT0/P63k (a), MWNT2/P63k (b) and MWNT6/P63k composites (c) with different concentrations of MWNT. The gap in the rheological experiments is about 0.9 mm.

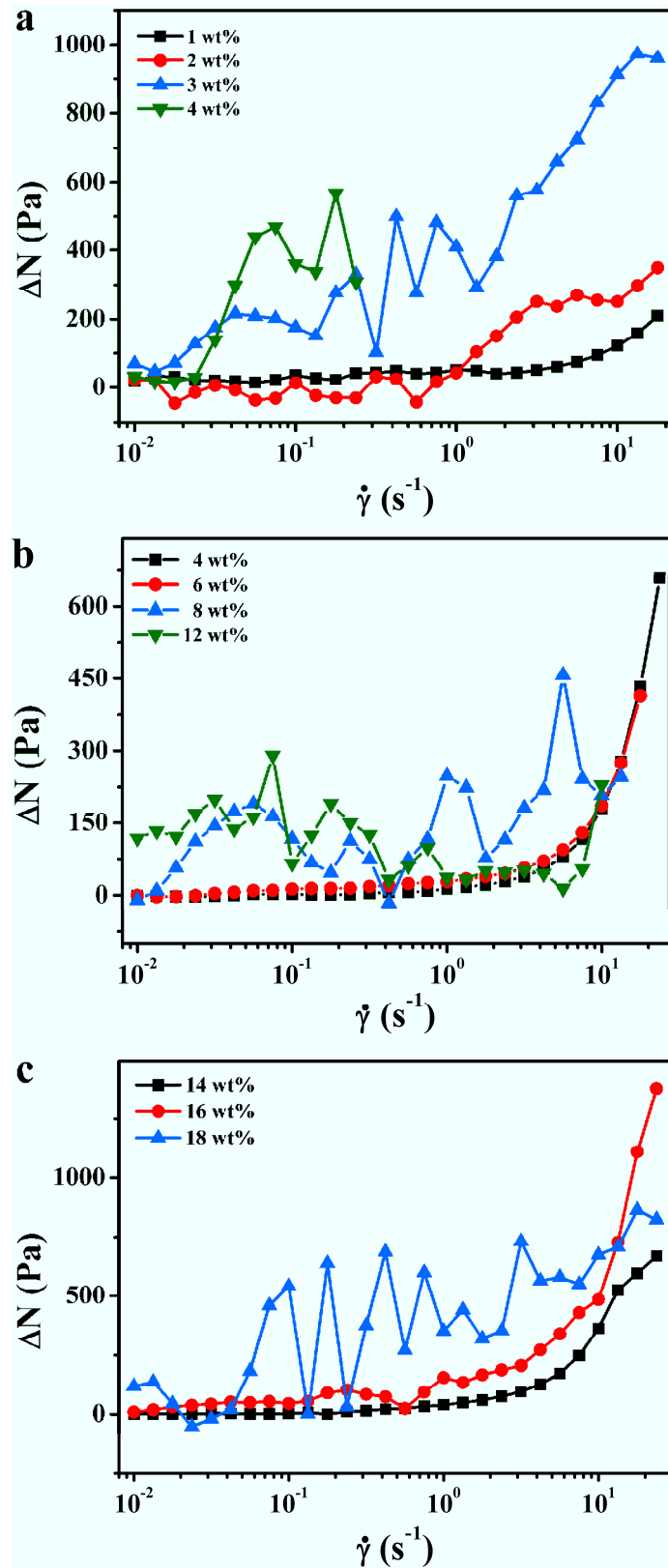


Fig. S18 Normal stress differences (ΔN) versus shear rate ($\dot{\gamma}$) for MWNT0/P117k (a), MWNT2/P117k (b) and MWNT6/P117k composites (c) with different concentrations of MWNT. The gap in the rheological experiments is about 0.9 mm.

Structural change under shear for MWNT/PDMS composites

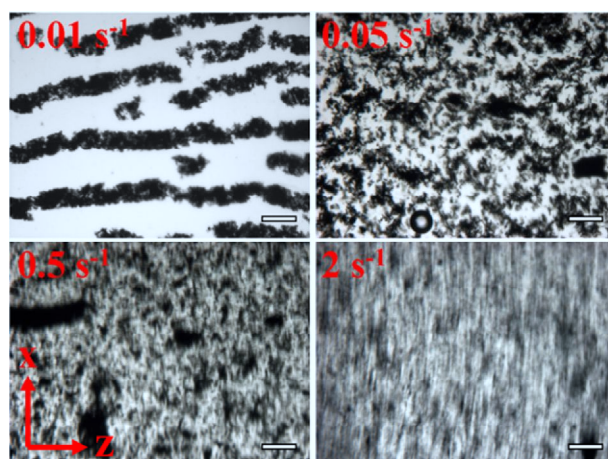


Fig. S19 Structures of 0.5 wt % MWNT0/P28k under different shear rates. The scale bars are $150 \mu\text{m}$ and the gap is $150 \mu\text{m}$. Photos are taken after shearing for about 45 s.

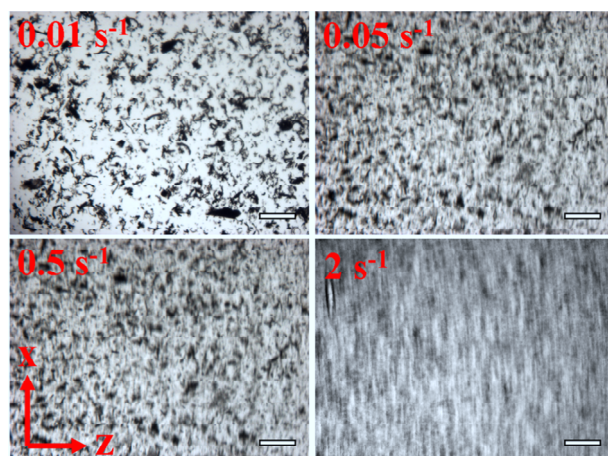


Fig. S20 Structures of 0.5 wt % MWNT0/P63k under different shear rates. The scale bars are $150 \mu\text{m}$ and the gap is $150 \mu\text{m}$. Photos are taken after shearing for about 45 s.

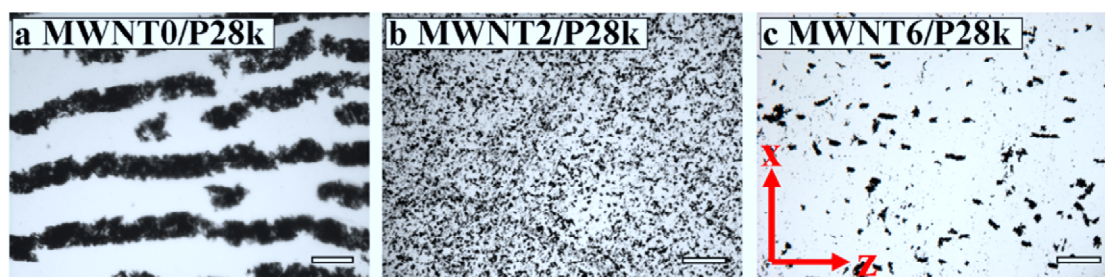


Fig. S21 Structures of 0.5 wt % MWNT0/P28k (a), 0.5 wt % MWNT2/P28k (b) and 0.5 wt % MWNT6/P28k (c) under a shear rate of 0.01 s^{-1} . The scale bars are $150 \mu\text{m}$ and the gap is $150 \mu\text{m}$. Photos are taken after shearing for about 45 s.

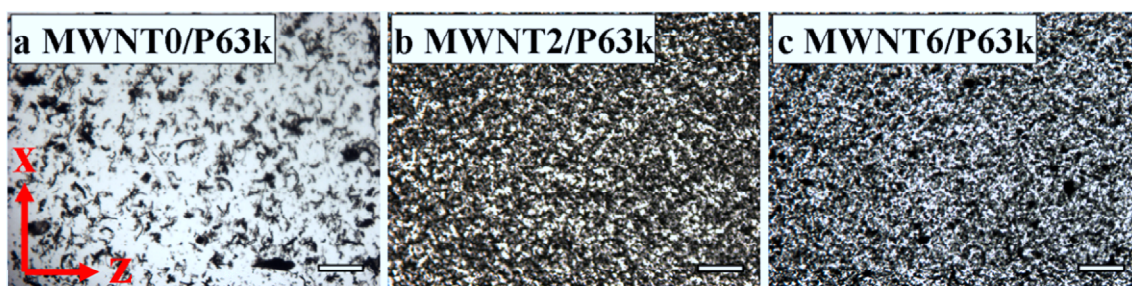


Fig. S22 Structures of 0.5 wt % MWNT0/P63k (a), 0.5 wt % MWNT2/P63k (b) and 0.5 wt % MWNT6/P63k (c) under a shear rate of 0.01 s^{-1} . The scale bars are $150 \mu\text{m}$ and the gap is $150 \mu\text{m}$. Photos are taken after shearing for about 45 s.



Fig. S23 Structures of 0.5 wt % MWNT0/P117k (a), 0.5 wt % MWNT2/P117k (b) and 0.5 wt % MWNT6/P117k (c) under a shear rate of 0.01 s^{-1} . The scale bars are $150 \mu\text{m}$ and the gap is $150 \mu\text{m}$. Photos are taken after shearing for about 45 s.

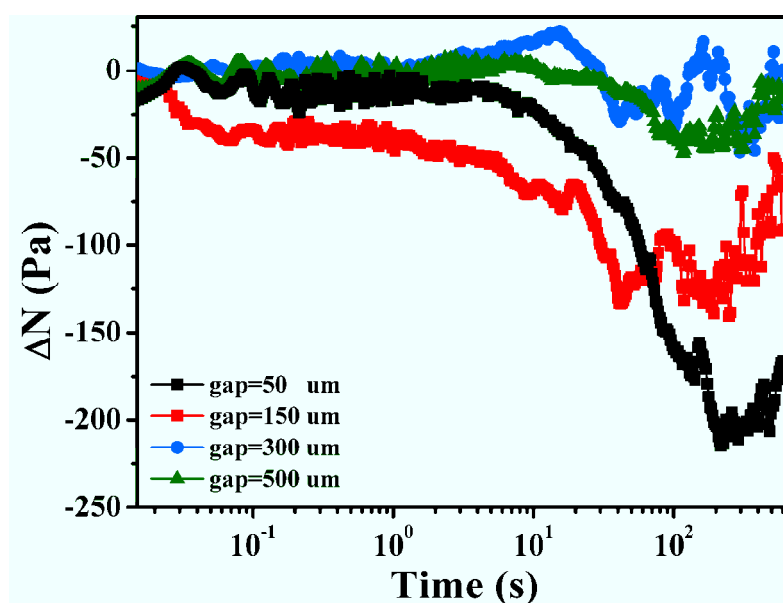


Fig. S24 Normal stress differences (ΔN) versus time at $\dot{\gamma} = 0.01 \text{ s}^{-1}$ for 1 wt % MWNT0/P28k under the gap of 50, 150, 300 and 500 μm .

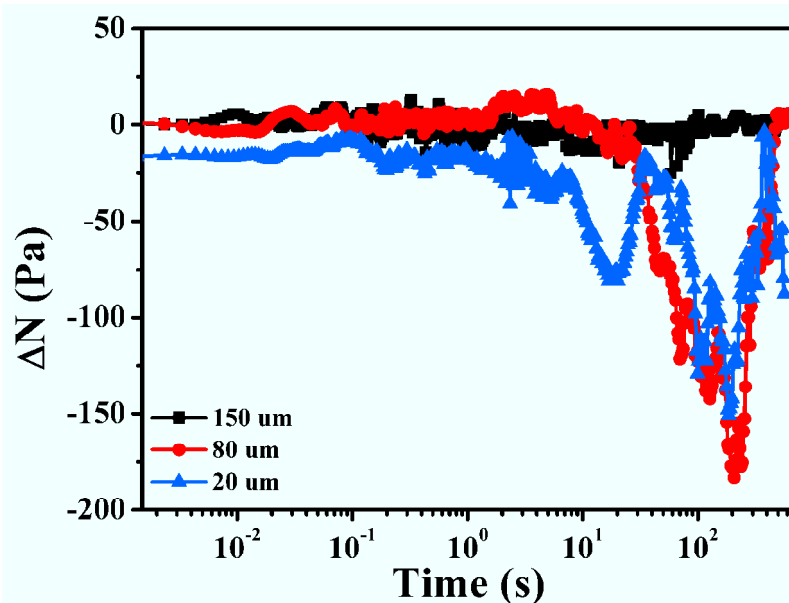


Fig. S25 Normal stress differences (ΔN) versus time at $\dot{\gamma} = 0.01 \text{ s}^{-1}$ for 0.5 wt % MWNT0/P63k under the gap of 150, 80 and 20 μm .

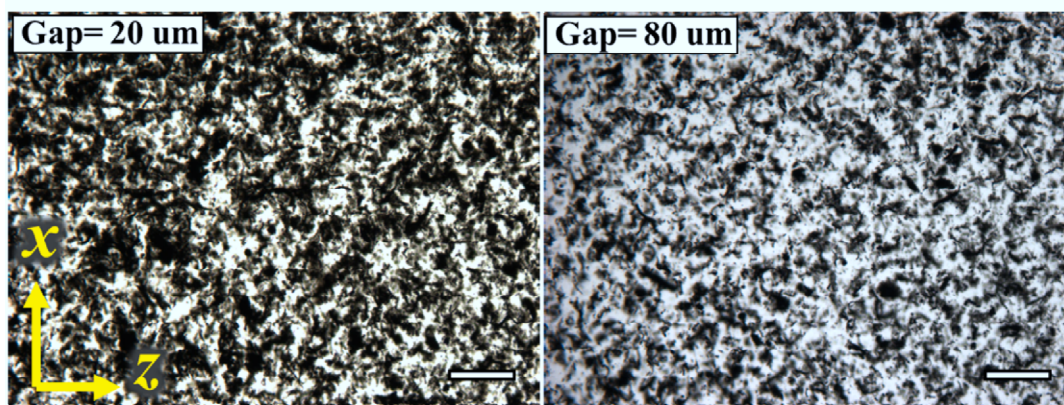


Fig. S26 Structures of 0.5 wt % MWNT0/P117k with the gap of 80 and 20 μm at a shear rate of 0.01 s^{-1} . The scale bars are 150 μm . Photos are taken after shearing for 150 s.

Average aggregate size of MWNTs in MWNT/PDMS composites

Table S1 Mean aggregate size of 0.5 wt % MWNT/PDMS composites

MWNT0/PDMS	R_0 (μm)	MWNT2/PDMS	R_0 (μm)	MWNT6/PDMS	R_0 (μm)
MWNT0/P6k	96.2	MWNT2/P6k	26.5	MWNT6/P6k	19.0
MWNT0/P28k	66.4	MWNT2/P28k	22.4	MWNT6/P28k	16.8
MWNT0/P63k	48.9	MWNT2/P63k	19.9	MWNT6/P63k	9.1
MWNT0/P117k	30.4	MWNT2/P117k	9.7	MWNT6/P117k	7.5

Table S2 Mean aggregate size of 2 wt % MWNT2/PDMS and 4 wt % MWNT6/PDMS composites

2 wt % MWNT2/PDMS	R_0 (μm)	4 wt % MWNT6/PDMS	R_0 (μm)
2 wt % MWNT2/P6k	68.4	4 wt % MWNT6/P6k	50.3
2 wt % MWNT2/P28k	58.1	4 wt % MWNT6/P28k	44.6
2 wt % MWNT2/P63k	27.0	4 wt % MWNT6/P63k	36.3
2 wt % MWNT2/P117k	20.1	4 wt % MWNT6/P117k	17.6

Steady shear results of pure PDMS

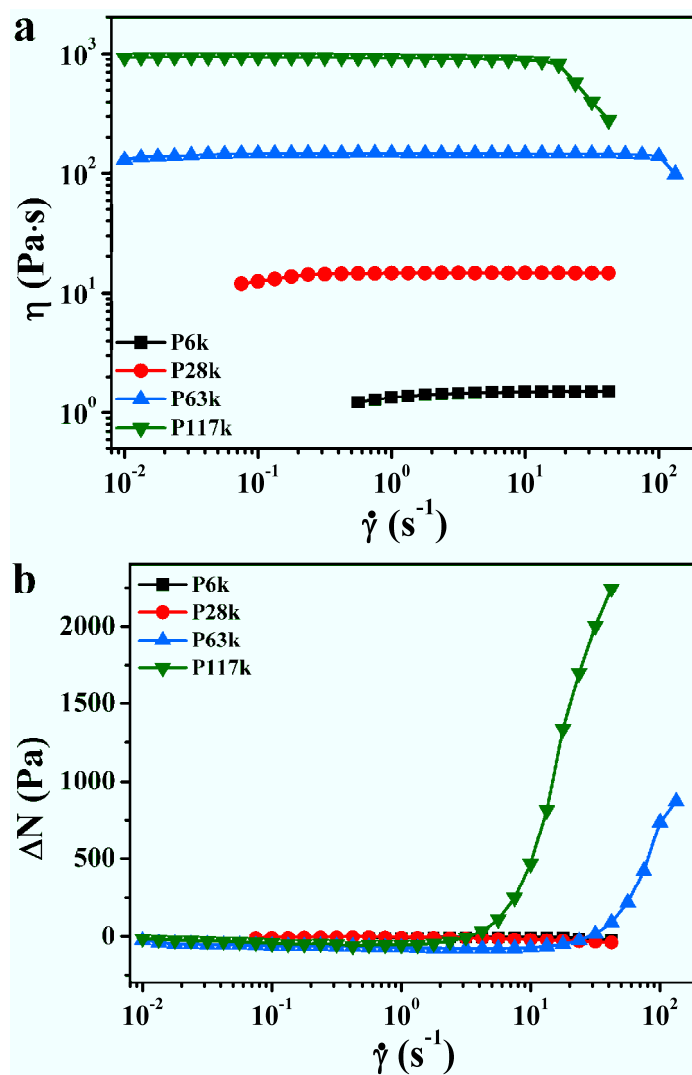


Fig. S27 Viscosity (a) and normal stress differences (b) versus shear rate for pure PDMS with different molecular weights. The gap in the rheological experiments is about 0.9 mm.

S1 K. Nishinari, *Prog. Colloid Polym. Sci.*, 2009, **136**, 87–94.

S2 R. Krishnamoorti and E. P. Giannelis, *Macromolecules*, 1997, **30**, 4097–4102.

S3 A. K. Kota, B. H. Cipriano, M. K. Duesterberg, A. L. Gershon, D. Powell, S. R. Raghavan and H. A. Bruck, *Macromolecules*, 2007, **40**, 7400–7406.